

# Contingency Constrained Planning with MPPI within MPPI

**Leonard Jung**

**Alexander Estornell**

**Michael Everett**

*Northeastern University, Boston, MA 02215, USA*

JUNG.LE@NORTHEASTERN.EDU

ESTORNELL.A@NORTHEASTERN.EDU

M.EVERETT@NORTHEASTERN.EDU

**Editors:** N. Ozay, L. Balzano, D. Panagou, A. Abate

## Abstract

For safety, autonomous systems must be able to consider sudden changes and enact contingency plans appropriately. State-of-the-art methods currently find trajectories that balance between nominal and contingency behavior, or plan for a singular contingency plan; however, this does not guarantee that the resulting plan is safe for all time. To address this research gap, this paper presents Contingency-MPPI, a data-driven optimization-based strategy that embeds contingency planning inside a nominal planner. By learning to approximate the optimal contingency-constrained control sequence with adaptive importance sampling, the proposed method’s sampling efficiency is further improved with initializations from a lightweight path planner and trajectory optimizer. Finally, we present simulated and hardware experiments demonstrating our algorithm generating nominal and contingency plans in real time on a mobile robot.

**Code:** <https://github.com/neu-autonomy/Contingency-MPPI>

**Video of Experiments:** <https://www.youtube.com/watch?v=RsXih-potZc>

**Keywords:** Contingency planning, model-predictive control, data-driven optimization, robotics

## 1. Introduction

Autonomous systems in real environments need to be able to handle sudden major changes in the operating conditions. For example, a car driving on the highway may need to swerve to safety if a collision occurs ahead, or a humanoid robot may need to grab hold of a railing if its foot slips on the stairs. Since there may be only a fraction of a second to recognize and respond to such events, this paper aims to develop an approach for always ensuring a contingency plan is available and can be immediately executed, if necessary.

A key challenge in this problem is to ensure a contingency plan always exists, without impacting the nominal plan too much. In standard approaches, where the nominal planner does not account for contingencies, the system could enter states from which no contingency plan exists; this may be tolerable if the failure event never occurs while the system is in one of those states but could lead to major safety failures in the worst case. Kim et al. (2021) considered these backup plans by adding weighted terms to the cost function, which *encourage* staying out of these contingency-free areas, but does not have any guarantee. Alternatively, the methods of Alsterda and Gerdès (2021) and Chen et al. (2022) explicitly plan alternative trajectories through a branching scheme and optimize both a nominal and set of contingency trajectories simultaneously. However, again, these methods must balance between the nominal trajectory cost and the tree of backup plans. Chen et al. (2022); Li et al. (2023); Peters et al. (2024) all addressed risk-aware contingency planning with stochastic interactions with other agents; thus, these algorithms aim to minimize risk and cost

---

. Distribution Statement A. Approved for public release: distribution unlimited

over a tree of possible future scenarios, again only providing a balance between aggressive and safe behavior. Pek and Althoff (2021) proposed a method for generating fail-safe trajectories via convex optimization, but is limited to autonomous ground vehicles. Tordesillas et al. (2019) solved a contingency constrained problem by planning both an optimistic plan and a contingency plan that branches off to stay in known-free space. However, for more complicated safety requirements (e.g., a collection of safe regions that must remain reachable within a given time limit), the mixed integer programming problem proposed in that work becomes too expensive to solve in real time.

This leads to another important challenge: ensuring computational efficiency despite needing to generate both a nominal and a contingency plan from each state along the way. One approach would be to use exact reachability algorithms (e.g., Bansal et al., 2017a; Wang et al., 2020) to keep the planner out of contingency-free areas. However, computing the reachable sets is expensive, not strictly necessary, and would still require subsequently finding the contingency trajectories. Instead, this paper proposes to use an inexpensive contingency planner embedded inside the nominal planner. If the contingency planner finds a valid contingency plan, the nominal planner knows that state is acceptable, and the corresponding contingency plan is already available. Meanwhile, if the contingency planner fails to find a trajectory within a computation budget, the nominal planner can quickly (albeit conservatively) update its plans to avoid that state. To handle these discrete contingency events on top of generic nominal planning problems, our method, Contingency-MPPI, builds on model-predictive path integral (MPPI) control by Williams et al. (2018).

To summarize, this paper’s contributions include: (i) a planning algorithm that embeds contingency planning inside a nominal planner to ensure that a contingency plan exists from every state along the nominal plan, (ii) extensions of this planner using lightweight optimization problems to improve the sample-efficiency via better initial guesses, and (iii) demonstrations of the proposed method in simulated environments and on a mobile robot hardware platform to highlight the real-time implementation.

## 2. Problem Formulation

Denote a general nonlinear discrete-time system  $\mathbf{x}_{t+1} = f(\mathbf{x}_t, \mathbf{u}_t)$  with state,  $\mathbf{x}_t \in \mathbb{R}^{n_x}$ , and control,  $\mathbf{u}_t \in \mathbb{R}^{n_u}$  at time  $t$ . To indicate a trajectory, we use colon notation (e.g.,  $\mathbf{x}_{0:T} = \{\mathbf{x}_0, \mathbf{x}_1, \dots, \mathbf{x}_T\}$ ) and  $T$ -step dynamics  $\mathbf{x}_{t+T} = f(\mathbf{x}_t, \mathbf{u}_{0:T})$ . Additionally  $\mathbf{U} \in \mathbb{R}^{n_u T}$  and  $\mathbf{X} \in \mathbb{R}^{n_x T}$  indicate the state and control trajectory reshaped into a vector, and  $\Sigma \in \mathbb{R}^{n_u T \times n_u T}$  represents the covariance matrix of the reshaped control trajectory.

The contingency-constrained planning problem is to find a nominal trajectory,  $\mathbf{u}_{0:T}$ , to minimize cost  $J_{\text{nom}}$ , along with contingency trajectories  $\{\mathbf{u}_{0:T_c}^0, \dots, \mathbf{u}_{0:T_c}^T\}$  that drive the system into a safe set,  $\mathcal{S}$ , within  $T_c$  steps, from each state along the nominal trajectory:

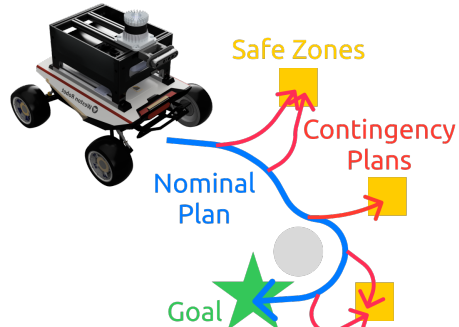


Figure 1: At each step along the nominal plan, a contingency plan must exist to reach a safe state within a time horizon.

$$\min_{\mathbf{u}_{0:T}, \{\mathbf{u}_{0:T_c}^0, \dots, \mathbf{u}_{0:T_c}^T\}} J_{\text{nom}}(\mathbf{x}_0, \mathbf{u}_{0:T}) \quad (1a)$$

$$\text{s.t.} \quad \mathbf{x}_{t+1} = f(\mathbf{x}_t, \mathbf{u}_t) \quad \forall t \in [0, \dots, T] \quad (1b)$$

$$\exists \tau \leq T_c \text{ s.t. } f(\mathbf{x}_i, \mathbf{u}_{0:\tau}^i) \in \mathcal{S} \quad \forall i \in [0, \dots, T]. \quad (1c)$$

Here, we assume that the safe set is predefined and static, representing contingency scenarios such as pulling off to the shoulder of a highway, or hiding from an seeking agent behind a tree. Other common costs/constraints (e.g., obstacle avoidance, control limits), can be added as desired.

### 3. Contingency-MPPI

Ignoring the contingency constraint Eq. (1c), MPPI is a powerful method for solving Eq. (1) when the dynamics or costs are non-convex. This section shows how to extend MPPI to handle Eq. (1c) as well, by nesting another sampling process into MPPI. First, we review the vanilla MPPI algorithm in Section 3.1, then describe our Nested-MPPI in Section 3.2. To increase sampling efficiency, a path-finding and trajectory optimization step (Section 3.3) is used to seed Nested-MPPI (Section 3.4) with ancillary controllers. This approach is summarized in Fig. 2.

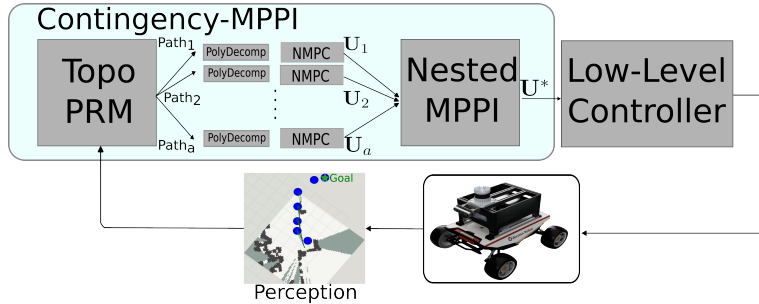


Figure 2: Planning Pipeline. Our Contingency-MPPI first runs (1) TopoRPM to find multiple paths through the environment (Section 3.3.1), (2) NMPC to find control sequences for each path (Section 3.3.2), and (3) Nested-MPPI that utilizes these control sequences as modes (Section 3.2) to find a trajectory for the vehicle to track.

#### 3.1. Background: Model Predictive Path Integral Control

To summarize MPPI following Asmar et al. (2023), consider the entire control trajectory as a single input  $\mathbf{V} \sim \mathcal{N}(\mathbf{U}, \Sigma)$ , sampled from distribution  $\mathbb{Q}$  with density

$$q(\mathbf{V}) = ((2\pi)^{n_u T} |\Sigma|)^{-\frac{1}{2}} e^{-\frac{1}{2}(\mathbf{V}-\mathbf{U})^T \Sigma^{-1} (\mathbf{V}-\mathbf{U})}, \quad (2)$$

where  $\mathbf{U}, \Sigma$  are the mean and covariance of  $\mathbb{Q}$ . The objective of MPPI is to minimize the KL-divergence between this proposed distribution,  $\mathbb{Q}$ , and an (unknown) optimal control distribution  $\mathbb{Q}^*$ , defined with respect to a cost function of the form

$$\mathcal{J}(\mathbf{X}, \mathbf{U}) = \mathbb{E}_{\mathbb{Q}}[\phi(\mathbf{X}) + c(\mathbf{X}) + \frac{\lambda}{2} \mathbf{U}^T \Sigma^{-1} \mathbf{U}]. \quad (3)$$

where  $\phi(\mathbf{X})$  and  $c(\mathbf{X})$  represent the state-dependent terminal and running cost, respectively. The optimal control distribution  $\mathbb{Q}^*$  has density  $q^*(\mathbf{V}) = \frac{1}{\eta}(-\frac{1}{\lambda}S(\mathbf{V}))p(\mathbf{V})$ , based on a state-dependent cost,  $S(\mathbf{V}) = \phi(\mathbf{X}) + c(\mathbf{X})$  and a nominal control distribution,  $\mathbb{P}$ , with density

$$p(\mathbf{V}) = ((2\pi)^{n_u T} |\Sigma|)^{-\frac{1}{2}} e^{-\frac{1}{2}(\mathbf{V} - \tilde{\mathbf{U}})^T \Sigma^{-1} (\mathbf{V} - \tilde{\mathbf{U}})}. \quad (4)$$

Here,  $\eta$  is a normalizing constant,  $\lambda$  is the inverse temperature, and  $\tilde{\mathbf{U}}$  is the base control, which is usually either zero or a nominal distribution from iterations of adaptive importance sampling. Then, to find the optimal control trajectory we can minimize the KL-divergence between  $\mathbb{Q}$  and  $\mathbb{Q}^*$ . Using adaptive importance sampling, the optimal control can be approximated by drawing  $K$  samples from a distribution  $\mathbb{Q}_{\hat{\mathbf{U}}}$  with proposed input  $\hat{\mathbf{U}}$ ,

$$\mathbf{U}^* = \mathbb{E}_{\mathbb{Q}}[w(\mathbf{V})\mathbf{V}], \quad (5)$$

$$w(\mathbf{V}) = \frac{1}{\eta} e^{-\frac{1}{\lambda}(S(\mathbf{V}) + \lambda(\hat{\mathbf{U}} - \tilde{\mathbf{U}})^T \Sigma^{-1} \mathbf{V})} \quad (6)$$

$$\eta = \int e^{-\frac{1}{\lambda}(S(\mathbf{V}) + \lambda(\hat{\mathbf{U}} - \tilde{\mathbf{U}})^T \Sigma^{-1} \mathbf{V})} d\mathbf{V}. \quad (7)$$

(5) finds an (information-theoretic) optimal open-loop control sequence that can be implemented in a receding horizon by shifting one timestep ahead and re-running the algorithm. As in Asmar et al. (2023), we weigh the control cost by a factor  $\gamma = \lambda(1 - \alpha)$  and shift all sampled trajectory costs by the minimum sampled cost, for numerical stability.

### 3.1.1. ENFORCING HARD CONSTRAINTS IN MPPI

While MPPI does not explicitly handle constraints, such as avoiding obstacles or the existence of a contingency plan, one can add terms to the objective with infinite cost when constraints are violated. For example, with a nominal cost  $S_{\text{nom}}(\mathbf{V})$  and  $N$  constraints, the augmented cost is  $S(\mathbf{V}) = S_{\text{nom}}(\mathbf{V}) + \sum_{k=1}^K S_{\text{constraint}}^k(\mathbf{V})$ , where

$$S_{\text{constraint}}^k(\mathbf{V}) = \begin{cases} 0, & \text{if constraint } k \text{ is satisfied} \\ \infty, & \text{o.w.} \end{cases}. \quad (8)$$

When the constraints are satisfied, the trajectory cost (and its weight in importance sampling) depends only on the nominal cost, such as minimum time or distance to the goal. If the constraints are not satisfied, the trajectory has infinite cost and receives zero weight in importance sampling. Thus, only trajectories meeting all constraints are considered, and their weights depend solely on the nominal cost. If no trajectory satisfies all constraints in an iteration, all samples get zero weight, and the mean control trajectory remains unchanged for the next MPPI iteration.

## 3.2. Nested-MPPI

This section introduces Nested-MPPI, which is summarized in Algorithm 1. This algorithm is based on the MPPI in Alsterda and Gerdes (2021) and allows for ancillary controllers as proposed in Trevisan and Alonso-Mora (2024). Our key innovation begins on Line 13, where a second level of MPPI executes in each state along each rollout of the nominal MPPI. This second level, described in Algorithm 2, optimizes for a contingency plan (with a different cost function than the nominal plan) as a way of evaluating the reachability constraint, Eq. (1c).

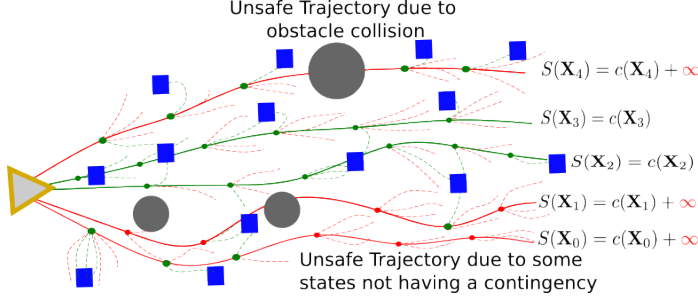


Figure 3: Nested-MPPI computes reachability cost by sampling contingency trajectories (dashed lines) along nominal trajectory rollouts (solid lines). Nominal trajectories 0, 1, and 4 collided with an obstacle or did not find a valid contingency from every state, and thus have  $+\infty$  cost.

<b>Algorithm 1:</b> Nested-MPPI	<b>Algorithm 2:</b> FindContingencyPlan
<b>1</b> <b>Input:</b> $\mathbf{x}_0, \mathbf{U}, [\mathbf{U}_a], \Sigma$	<b>1</b> <b>Input:</b> $X$ : State sequence
<b>2</b> <b>Output:</b> Nom. & contingency control seqs	<b>2</b> <b>Output:</b> Contingency control seq. & score
<b>3</b> <b>Parameters:</b> $K, T, L$ (nominal); $f, G$ , (system); $c, \phi, \lambda, \alpha$ (cost)	<b>3</b> <b>Parameters:</b> $K_c, T_c, L_c, T_s$ (contingency); $f, G, m_{\text{elite}}$ (system/sampling); $\varepsilon, \lambda, \alpha$ (costs)
<b>4</b> $\mathbf{U}' \leftarrow \mathbf{U}; \Sigma' \leftarrow \Sigma$	<b>4</b> $\mathbf{U}' \leftarrow \mathbf{0}$
<b>5</b> <b>for</b> $l \leftarrow 0$ <b>to</b> $L - 1$ <b>do</b> // AIS loop	<b>5</b> <b>for</b> $i \leftarrow 0$ <b>to</b> $T_s - 1$ <b>do</b>
<b>6</b> <b>for</b> $k \leftarrow 0$ <b>to</b> $K - 1 + \text{card}([\mathbf{U}_a])$ <b>do</b>	<b>6</b> <b>for</b> $l \leftarrow 0$ <b>to</b> $L_c - 1$ <b>do</b>
<b>7</b> $\mathbf{x}_{k,0} \leftarrow \mathbf{x}_0$	<b>7</b> $\mathbf{x} \leftarrow \mathbf{x}_i$
<b>8</b> $\mathcal{E}_k \sim \mathcal{N}(0, \Sigma')$	<b>8</b>
<b>9</b> <b>if</b> $k \leq K - 1$ <b>then</b> $\mathbf{U} = \mathbf{U}' + \mathcal{E}_k$ // Ancillary Control	<b>9</b>
<b>10</b> <b>else</b> $\mathbf{U} = [\mathbf{U}_a]_{k-(K-1)}$	<b>10</b>
<b>11</b> <b>for</b> $i \leftarrow 0$ <b>to</b> $T - 1$ <b>do</b>	<b>11</b>
<b>12</b> $\mathbf{x}_{k,i+1} = \mathbf{x}_{k,i} + (f + G(\mathbf{u})) \Delta t$	<b>12</b>
<b>13</b> $\mathbf{U}_{\text{reach}_k}, S_{\text{reach}} \leftarrow$ FindContingencyPlan( $\mathbf{X}_k$ )	<b>13</b>
<b>14</b> <b>if</b> $S_{\text{reach}} = 0$ <b>then</b>	<b>14</b>
<b>15</b> $\mathbf{U}_{\text{contingency}} \leftarrow \mathbf{U}_{\text{reach}_k}$	<b>15</b>
<b>16</b> $S_k \leftarrow S_{\text{reach}} + c(\mathbf{X}) + \phi(\mathbf{X}) +$ $\lambda(1 - \alpha)\mathbf{U}'^T \Sigma^{-1}(\mathcal{E}_k + \mathbf{U}' - \mathbf{U})$	<b>15</b>
<b>17</b> <b>if</b> $l < L - 1$ <b>then</b> $\mathbf{U}', \Sigma' \leftarrow \text{AIS}()$	<b>16</b>
<b>18</b> $\rho \leftarrow \min(\mathbf{S})$	<b>16</b>
<b>19</b> $\eta \leftarrow \sum_{k=1}^K \exp(-\frac{1}{\lambda}(S_k - \rho))$	<b>17</b>
<b>20</b> $\mathbf{U} +=$ $\frac{1}{\eta} \exp(-\frac{1}{\lambda}(S_k - \rho)) (\mathcal{E}_k + \mathbf{U}' - \mathbf{U})$	<b>17</b>
<b>21</b> <b>return</b> $\mathbf{U}, \mathbf{U}_{\text{contingency}}$	<b>18</b> <b>return</b> $\mathbf{U}', \sum_{i=0}^{T_s-1} S_{i,\text{reach}}$

To both find contingency trajectories and evaluate whether the reachability constraint (1c) is satisfied for any control sequence, we first roll out each control sequence  $\mathbf{U}_i$  by passing it through the zero-noise nonlinear dynamics model to get the state sequence  $\mathbf{X}_i$ . Then, at each state  $\mathbf{x}_t$  for  $t = 0, \dots, T_s - 1$ , we run  $L_c$  rounds of adaptive importance sampling MPPI with  $N_c$  samples and  $T_c$  timesteps starting at  $\mathbf{x}_t$  to generate contingency state  $[\mathbf{X}_0^s, \dots, \mathbf{X}_{L \times N_c}^s]$  and control  $[\mathbf{U}_0^s, \dots, \mathbf{U}_{L \times N_c}^s]$  trajectories (lines 6-16 in Alg. 2). Here,  $T_s$  is the number of timesteps along the nominal (solid lines in Fig. 3) to check the contingency condition, and  $T_c$  is the safety horizon to satisfy the contingency condition. To encourage these contingency trajectories to reach safe states within  $T_c$  timesteps, we use state-dependent cost

$$c_{\text{contingency}}(\mathbf{X}^s) = \min_{\zeta \in \mathcal{S}, \mathbf{x} \in \mathbf{X}^s} \|\mathbf{x} - \zeta\|. \quad (9)$$

Then, as seen in Figure 3, if any of the contingency trajectories successfully reaches a state within an  $\varepsilon$  ball of a safe state within  $T_c$  timesteps, we mark that state  $\mathbf{x}_t$  along  $\mathbf{X}_i$  as safe (green). If all states along  $\mathbf{X}_i$  are marked as safe, then we mark  $\mathbf{X}_i$  and its corresponding control  $\mathbf{U}_i$  as safe; otherwise, we mark the trajectory as unsafe, and add  $+\infty$  to its corresponding cost. In Algorithm 2 Line 9, to initialize the proposed distribution for contingencies at each state, a number of sample control trajectories are drawn from a uniform distribution along control bounds  $\mathbf{u}_{t,0:T_c} \sim U(\mathbf{u}_{lb}, \mathbf{u}_{ub})$ , and the cross-entropy method is used on the best  $m$  trajectories to determine an initial mean and covariance.

### 3.3. Improving the Sampling Efficiency of Nested-MPPI: Frontend

Although Algorithm 1 considers all costs and constraints from Eq. (1), the sampling process can result in many or even all trajectories with infinite costs (if the sampling distribution is far from the optimal distribution), which leads to uninformed updates to the distribution. To remedy this, one may simply sample more  $\mathbf{U}$  sequences; however, each additional sequence requires computing  $S_{\text{reach}}$ , which requires an additional  $T_s$  MPPI computations. Instead, we propose to approximate locally optimal  $\mathbf{U}$  and consider them as a new sampling distribution(s) into Algorithm 1, as described in Section 3.4. First, we find several different paths between the start and goal. For each path, we then perform a convex decomposition to find an under approximation of the safe space, and finally perform a nonlinear MPC to solve for a candidate control sequence.

#### 3.3.1. TOPO-PRM

To find several alternative paths through the workspace, we leverage Topo-PRM proposed in Zhou et al. (2020). As Topo-PRM finds a collection of topologically distinct paths through the environment, our planner can "explore" the free-space and return multiple promising guiding paths. However as Topo-PRM does not consider safe zones, it may return paths that are not near safe zones, and thus no contingencies exist. Thus, we modify the algorithm to sample randomly from safe states  $p$  fraction of the time to bias our roadmap to find paths that include safe states. To further bias the paths towards safe zones, denoting  $V_{\max}$  as the maximum speed of our vehicle in the creation of our workspace occupancy grid, we add pseudo-obstacles by marking occupied voxels that are farther than  $r_{\max} = V_{\max} T_s \Delta t$  away from any given safe zone.

### 3.3.2. NONLINEAR MPC

To transform each path into an ancillary control trajectory, we first find the point  $E$  that is  $r_{\max}$  along the path, and then perform a convex decomposition using the approach from Liu et al. (2017) of the free space along the path from our start point  $S$  to  $E$ . Next, we find  $M$  knot points by discretizing  $M - 1$  points along the path from  $S$  to  $E$ . Denoting  $A_i \mathbf{p} < b_i$  the polyhedral constraint in which point  $p_i$  lies within, we solve the following nonlinear programming problem to recover a candidate ancillary control trajectory:

$$\begin{aligned} U_{\text{anci}} = \arg \min_{\mathbf{X}, \mathbf{U}} & \sum_{i=0}^N \|\mathbf{x}_i - \mathbf{x}_{goal}\| \\ \text{s.t. } & A_i \beta \mathbf{x}_i < b_i \\ & \mathbf{x}_{i+1} = f(\mathbf{x}_i, \mathbf{u}_i) \forall i \in \{0, M\} \\ & \mathbf{x}_0 = \mathbf{x}_{start}, \end{aligned} \quad (10)$$

where  $\beta \in \mathbb{R}^{n_x \times n_x}$  selects elements of the state space present in the workspace (i.e.,  $\mathbf{p}_i = \beta \mathbf{x}_i$ ).

### 3.4. Improving the Sampling-Efficiency of Nested-MPPI: Backend

To use each of the control sequences found in Section 3.3, we sample around the control sequences and insert the resulting set of samples as biases to MPPI as in Trevisan and Alonso-Mora (2024). As seen in Alg. 3, we append each of the  $B$  control sequences from MPC to a list of ancillary control sequences,  $[U_a]$ . Then, in Alg. 1 Line 10, each ancillary control sequence  $U_a$  is used as a mean for an individual distribution,  $\mathcal{V} \sim \mathcal{N}(U_a, \Sigma)$ , where  $\Sigma$  is the current covariance of our MPPI algorithm, and sample  $N_a$  samples. For the rest of the  $N - B \cdot N_a$  samples the current MPPI running mean is used (Algorithm 1 Lines 9). Intuitively, this is equivalent to inserting each bias as a mode in a Gaussian mixture model.

---

**Algorithm 3: Contingency-MPPI**


---

```

1 Input:  $\mathbf{x}_s, \mathbf{x}_g, U_{init}, \Sigma$ 
2 Output: Nominal & contingency control
   sequences
3 Parameters:  $f, G$ , (system);  $\mathcal{S}, O$ ,
   (environment)
4 while task not completed do
5    $P_x, P_y \leftarrow \text{Topo-PRM}(\mathbf{x}, \mathcal{S}, O)$ 
6   for  $s \leftarrow 0$  to  $B$  do
7      $\mathbf{A}, \mathbf{b} \leftarrow \text{PolyDecomp}(O);$ 
8      $\mathbf{U}_{\text{anci}} \leftarrow \text{NMPC}(f, G, \mathbf{A}, \mathbf{b})$  for
9        $n \leftarrow 0$  to  $N_a$  do
10       $\mathcal{V} \sim \mathcal{N}(\mathbf{U}_{\text{anci}}, \Sigma)$ 
11       $[U_a].append(\mathcal{V})$ 
12    $\mathbf{U}, \mathbf{U}_{\text{contingency}} \leftarrow$ 
13   Nested-MPPI( $\mathbf{x}_s, U_{init}, [U_a], \Sigma_{init}$ )
14 return  $\mathbf{U}, \mathbf{U}_{\text{contingency}}$ 

```

---

## 4. Experiments

We demonstrate Contingency-MPPI on a hide-and-seek task in both simulation and hardware to highlight its ability to (1) ensure a contingency plan exists at all time and (2) run in real-time within an autonomy stack. Critically, our results show that Contingency-MPPI not only guarantees the existence of contingencies but computes the trajectories as well. At a moment's notice, our planner can switch to its contingency behavior without needing to replan a new trajectory.

	AIS-MPC	MPC	Base	MPPI	MPPI-H	MPPI-MPC
Reached Goal Rate (%) $\uparrow$	100	100	0.0	100	100	100
Unsafe Problems (%) $\downarrow$	0.0	0.0	0.0	41	31	9
Average Timestep To Goal $\downarrow$	65.7	66.7	N/A	66.7	69.3	58.3
Finite Cost Sampling (%) $\uparrow$	78.1	77.8	91.2	N/A	N/A	N/A

Table 1: Simulation Results over 150 environments. Each environment generated was checked to ensure a valid solution exists

#### 4.1. Implementation Details

As discussed in Asmar et al. (2023), multiple adaptive importance sampling methods may be used; we chose to use the cross-entropy method for its simplicity and speed. To enable real-time computation, each iteration of lines 6-15 in Alg. 1 is batched using JAX (Bradbury et al., 2018). Additionally, each iteration of lines 5-17 and 8-14 in Alg. 2 are also batched. Thus, the Nested-MPPI algorithm run time scales roughly by  $L(T + L_s(T_c))$ . For longer time horizons, we treated the control sequence and state sequence as a reference trajectory for a lower-level controller (iLQG, Todorov and Li, 2005) to track. To solve the shooting NMPC problem, we used CasADi (Andersson et al., 2019) and SNOPT (Gill et al., 2005).

#### 4.2. Hide and Seek

The experimental environment consists of several safe positions  $p = [x, y]$ , a start pose, an end position, and several obstacles. The objective is to control a differential-drive car from the start pose to the end position in minimum time, while satisfying the reachability constraint. Thus, the nominal cost is

$$c_{\text{nom}}(\mathbf{X}) = \sum_{t=0}^{T-1} (\mathbf{x}_t - \mathbf{x}_{\text{goal}})^T \mathbf{Q} (\mathbf{x}_t - \mathbf{x}_{\text{goal}}). \quad (11)$$

We assume the location of safe positions is known, but the robot has a limited sensing horizon and thus operates with unknown obstacles. To handle this, an additional constraint is added to the cost function:

$$c_{\text{known}}(\mathbf{X}) = \begin{cases} 0 & \mathbf{x} \text{ exists in known space } \forall t \in \{0, \dots, T_{\text{safe}} - 1\} \\ \infty & \text{o.w} \end{cases}, \quad (12)$$

which ensures all states  $i = 0, \dots, T_{\text{safe}}$  in the nominal trajectories remain in the known region.

#### 4.3. Simulation Results

We ran 3 baseline algorithms and 3 variants of our algorithm against a set of 150 randomly generated problems: the MPPI algorithm is the original Asmar et al. (2023) MPPI with AIS algorithm considering only the nominal cost, and not the reachability safety constraint; The MPPI-H algorithm is MPPI with an additional running cost term  $30 * \min_{\zeta \in \mathcal{S}} (\|\mathbf{x}_t - \zeta\|)$ ; the MPPI-MPC is the MPPI-H algorithm with MPC seeding; Base algorithm is the Nested-MPPI algorithm; MPC includes MPC seeding with Nested-MPPI; AIS-MPC additionally considers adaptive importance sampling for the branching contingency control trajectories. Over the trials, we present the average Reached Goal

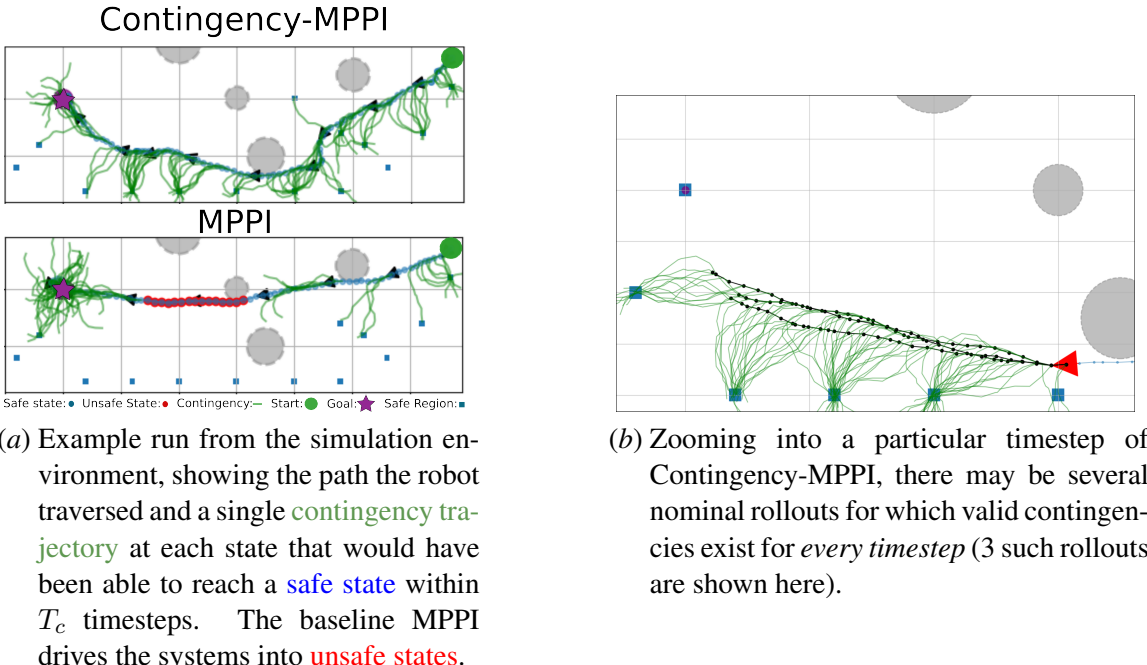


Figure 4: Comparison of Contingency-MPPI results.

Rate (percentage of trials where the vehicle reached the goal position), Unsafe Problems (percentage of trials where at least one state had no valid contingency), Average Timestep to Goal, and Average Finite Cost Sampling Percentage (at each timestep, the percentage of sampled trajectories that satisfied the contingency condition). To evaluate the Unsafe Problems metric we ran Bansal et al. (2017b) offline after each trial along the resultant trajectory to determine whether a safe zone was reachable from each state. All the variants of our algorithm used a planning horizon of  $T = 30$ ,  $T_s = 30$ ,  $T_c = 15$ , sampling size of  $K = 100$ ,  $K_c = 100$ , AIS iterations  $L = L_c = 3$ ,  $m_{\text{elite}} = 5$  and  $\varepsilon = 0.5$ . Baseline variants had planning horizon  $T = 30$ , with higher sampling size  $K = 1000$ . All variants had  $\lambda = 0.1$  and  $\alpha = 0$ , and were ran on an RTX 4090 with an Intel i9-13900K.

The proposed methods always provide a contingency path to a safe zone anywhere along its trajectory (0% unsafe problems), while all baseline variants enter unsafe states. Additionally, Table 1 highlights the advantage of using the topological NMPC frontend and AIS branched Contingency-MPPI in terms of successful solve, given the same sampling parameters. Using the MPC seeding helps both our algorithm and the baseline reach the goal quicker; however, only our algorithm provides a guarantee of safety at all timesteps. However this comes at an computational expense, as from Table 2, running the TopoPRM and NMPC algorithm consumes a majority of the runtime for one iteration of our Contingency-MPPI.

An example run in Fig. 4(a) compares AIS-MPC and vanilla MPPI. Our Contingency-MPPI always has a contingency trajectory to a safe zone, while the vanilla MPPI violates this safety

	Average Time (s)
NMPC	0.017
Nested-MPPI	0.012
TopoPRM	0.040
Total	0.069

Table 2: Sim Timing Results per Iteration of Contingency-MPPI

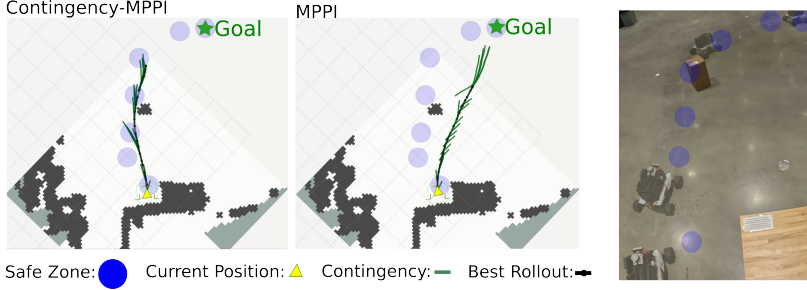


Figure 5: Example from Hardware Experiment. (Left) Best rollout for Contingency-MPPI vs MPPI at  $t = 0$  with contingency trajectories at each timestep. (Right) Snapshot view of robot executing Contingency-MPPI.

condition for several time steps. Fig. 4(b) provides a closer look at the rollouts under consideration at a particular timestep of AIS-MPC.

#### 4.4. Hardware Results

For the hardware experiments, we ran Contingency-MPPI on an Alienware Intel NUC 11 with an i7 processor and RTX 2060 GPU onboard our customized Agile-X Scout Mini platform with an Ouster OS1-32 3D lidar sensor. For robot localization and occupancy map creation, we ran direct lidar-inertial odometry (DLIO, Chen et al., 2023) on the same computer as the planner. A frame from an example trial is shown in Fig. 5 with video results in the supplementary material. Contingency-MPPI provides contingencies to the safe zones at every timestep along the nominal plan, while vanilla MPPI’s rollout does not. The hardware experiments were conducted at varying speeds from 1-3 m/s with a varying number of obstacles, and all trials were conducted without a prior obstacle map; thus, our algorithm was capable of running in unknown environments and in real time.

## 5. Summary

This paper presented a method to solve contingency-constrained planning problems, enforcing the existence of a finite-time contingency trajectory at all timesteps along our robot’s planned trajectory. The proposed algorithm, Contingency-MPPI, handles this constraint with adaptive importance sampling along each control trajectory. To improve sampling efficiency, the approach includes a separate MPC process to seed the MPPI modes. Finally, we demonstrate Contingency-MPPI both in simulation and hardware. Future work will consider high-dimensional dynamics and dynamic obstacles, where we expect the required sampling density to greatly increase. Similarly, we plan to investigate incorporating other types of contingency behaviors, such as lane weaving on a highway or staying close to a shoulder along a road.

## Acknowledgments

This work was supported by award W911NF-24-2-006.

## References

- John P Alsterda and J Christian Gerdes. Contingency model predictive control for linear time-varying systems. *arXiv preprint arXiv:2102.12045*, 2021.
- Joel A E Andersson, Joris Gillis, Greg Horn, James B Rawlings, and Moritz Diehl. CasADi – A software framework for nonlinear optimization and optimal control. *Mathematical Programming Computation*, 11(1):1–36, 2019. doi: 10.1007/s12532-018-0139-4.
- Dylan M Asmar, Ransalu Senanayake, Shawn Manuel, and Mykel J Kochenderfer. Model predictive optimized path integral strategies. In *2023 IEEE International Conference on Robotics and Automation (ICRA)*, pages 3182–3188. IEEE, 2023.
- Somil Bansal, Mo Chen, Sylvia Herbert, and Claire J. Tomlin. Hamilton-jacobi reachability: A brief overview and recent advances. In *2017 IEEE 56th Annual Conference on Decision and Control (CDC)*, pages 2242–2253, 2017a. doi: 10.1109/CDC.2017.8263977.
- Somil Bansal, Mo Chen, Sylvia Herbert, and Claire J Tomlin. Hamilton-jacobi reachability: A brief overview and recent advances. In *2017 IEEE 56th Annual Conference on Decision and Control (CDC)*, pages 2242–2253. IEEE, 2017b.
- James Bradbury, Roy Frostig, Peter Hawkins, Matthew James Johnson, Chris Leary, Dougal Maclaurin, George Necula, Adam Paszke, Jake VanderPlas, Skye Wanderman-Milne, and Qiao Zhang. JAX: composable transformations of Python+NumPy programs, 2018. URL <http://github.com/jax-ml/jax>.
- Kenny Chen, Ryan Nemiroff, and Brett T. Lopez. Direct lidar-inertial odometry: Lightweight lio with continuous-time motion correction. In *2023 IEEE International Conference on Robotics and Automation (ICRA)*, pages 3983–3989, 2023. doi: 10.1109/ICRA48891.2023.10160508.
- Yuxiao Chen, Ugo Rosolia, Wyatt Ubellacker, Noel Csomay-Shanklin, and Aaron D. Ames. Interactive multi-modal motion planning with branch model predictive control. *IEEE Robotics and Automation Letters*, 7(2):5365–5372, 2022. doi: 10.1109/LRA.2022.3156648.
- Philip E. Gill, Walter Murray, and Michael A. Saunders. Snopt: An sqp algorithm for large-scale constrained optimization. *SIAM Rev.*, 47(1):99–131, jan 2005. ISSN 0036-1445. doi: 10.1137/S0036144504446096. URL <https://doi.org/10.1137/S0036144504446096>.
- Hunmin Kim, Hyungjin Yoon, Wenbin Wan, Naira Hovakimyan, Lui Sha, and Petros Voulgaris. Backup plan constrained model predictive control. In *2021 60th IEEE Conference on Decision and Control (CDC)*, pages 289–294, 2021. doi: 10.1109/CDC45484.2021.9683388.
- Tong Li, Lu Zhang, Sikang Liu, and Shaojie Shen. Marc: Multipolicy and risk-aware contingency planning for autonomous driving. *IEEE Robotics and Automation Letters*, 2023.
- Sikang Liu, Michael Watterson, Kartik Mohta, Ke Sun, Subhrajit Bhattacharya, Camillo J. Taylor, and Vijay Kumar. Planning dynamically feasible trajectories for quadrotors using safe flight corridors in 3-d complex environments. *IEEE Robotics and Automation Letters*, 2(3):1688–1695, 2017. doi: 10.1109/LRA.2017.2663526.

Christian Pek and Matthias Althoff. Fail-safe motion planning for online verification of autonomous vehicles using convex optimization. *IEEE Transactions on Robotics*, 37(3):798–814, 2021. doi: 10.1109/TRO.2020.3036624.

Lasse Peters, Andrea Bajcsy, Chih-Yuan Chiu, David Fridovich-Keil, Forrest Laine, Laura Ferranti, and Javier Alonso-Mora. Contingency games for multi-agent interaction. *IEEE Robotics and Automation Letters*, 9(3):2208–2215, 2024. doi: 10.1109/LRA.2024.3354548.

E. Todorov and Weiwei Li. A generalized iterative lqg method for locally-optimal feedback control of constrained nonlinear stochastic systems. In *Proceedings of the 2005, American Control Conference, 2005.*, pages 300–306 vol. 1, 2005. doi: 10.1109/ACC.2005.1469949.

Jesus Tordesillas, Brett T Lopez, and Jonathan P How. Faster: Fast and safe trajectory planner for flights in unknown environments. In *2019 IEEE/RSJ international conference on intelligent robots and systems (IROS)*, pages 1934–1940. IEEE, 2019.

Elia Trevisan and Javier Alonso-Mora. Biased-mppi: Informing sampling-based model predictive control by fusing ancillary controllers. *IEEE Robotics and Automation Letters*, 2024.

Xinrui Wang, Karen Leung, and Marco Pavone. Infusing reachability-based safety into planning and control for multi-agent interactions. In *2020 IEEE/RSJ International Conference on Intelligent Robots and Systems (IROS)*, pages 6252–6259, 2020. doi: 10.1109/IROS45743.2020.9341499.

Grady Williams, Paul Drews, Brian Goldfain, James M Rehg, and Evangelos A Theodorou. Information-theoretic model predictive control: Theory and applications to autonomous driving. *IEEE Transactions on Robotics*, 34(6):1603–1622, 2018.

Boyu Zhou, Fei Gao, Jie Pan, and Shaojie Shen. Robust real-time uav replanning using guided gradient-based optimization and topological paths. In *2020 IEEE International Conference on Robotics and Automation (ICRA)*, pages 1208–1214, 2020. doi: 10.1109/ICRA40945.2020.9196996.